# Sensorless Field Oriented Control for a Permanent Magnet Synchronous Motor Using a PLL Estimator and Equation-based Flux Weakening



#### Introduction

Current industry trends suggest that the Permanent Magnet Synchronous Motor (PMSM) is one of the most preferred motors by motor control application designers. Its strengths, such as high-power density, fast dynamic response and high efficiency in comparison with other motors in its category, coupled with decreased manufacturing costs and improved magnetic properties, make the PMSM a good recommendation for large-scale product implementation.

Microchip provides a wide range of 16-bit and 32-bit microcontrollers (MCUs) for enabling efficient, robust and versatile control of all types of motors, along with reference designs of the necessary tool sets, resulting in a fast learning curve and a shortened development cycle for new products. For additional information on 32-bit MCUs for Motor Control, see Architectural Highlights of 32-bit MCUs for Motor Control Applications.

# **Table of Contents**

Int	troduction	
1.	Field Oriented Control (FOC)	
2.	PLL Type Estimator	
3.	Tuning and Experimental Results	1
4.	Equation-based Flux Weakening	1:
5.	Architectural Highlights of 32-bit MCUs for Motor Control Applications	10
	5.1. The SAM E70 Family of Devices	10
	5.2. The PIC32MK Family of Devices	
6.	Conclusion	18
7.	References	19
8.	Revision History	20
	8.1. Revision D (December 2024)	
	8.2. Revision C (August 2018)	
	8.3. Revision B (September 2017)	20
	8.4. Revision A (August 2017)	20
Mid	licrochip Information	2 <sup>-</sup>
	Trademarks	2 <sup>-</sup>
	Legal Notice	2 <sup>-</sup>
	Microchin Devices Code Protection Feature	<b>7</b> ·



# 1. Field Oriented Control (FOC)

In case of the PMSM, the rotor field speed must be equal to the stator (armature) field speed (i.e., synchronous). The loss of synchronization between the rotor and stator fields causes the motor to halt.

FOC represents the method by which one of the fluxes (rotor, stator, or air gap) is considered as a basis for creating a reference frame for one of the other fluxes with the purpose of decoupling the torque and flux-producing components of the stator current. The decoupling assures the ease of control for complex three-phase motors in the same manner as DC motors with separate excitation. This means the armature current is responsible for the torque generation, and the excitation current (for a PMSM motor, permanent magnet) is responsible for the flux generation. In this application note, the rotor flux is considered as a reference frame for the stator and air gap flux.

Several application notes from Microchip describe the principles behind FOC. Two such examples are (see References): "AN1078 - Sensorless Field Oriented Control of PMSM Motors" and "AN908 - Using the dsPIC30F for Vector Control of an ACIM".

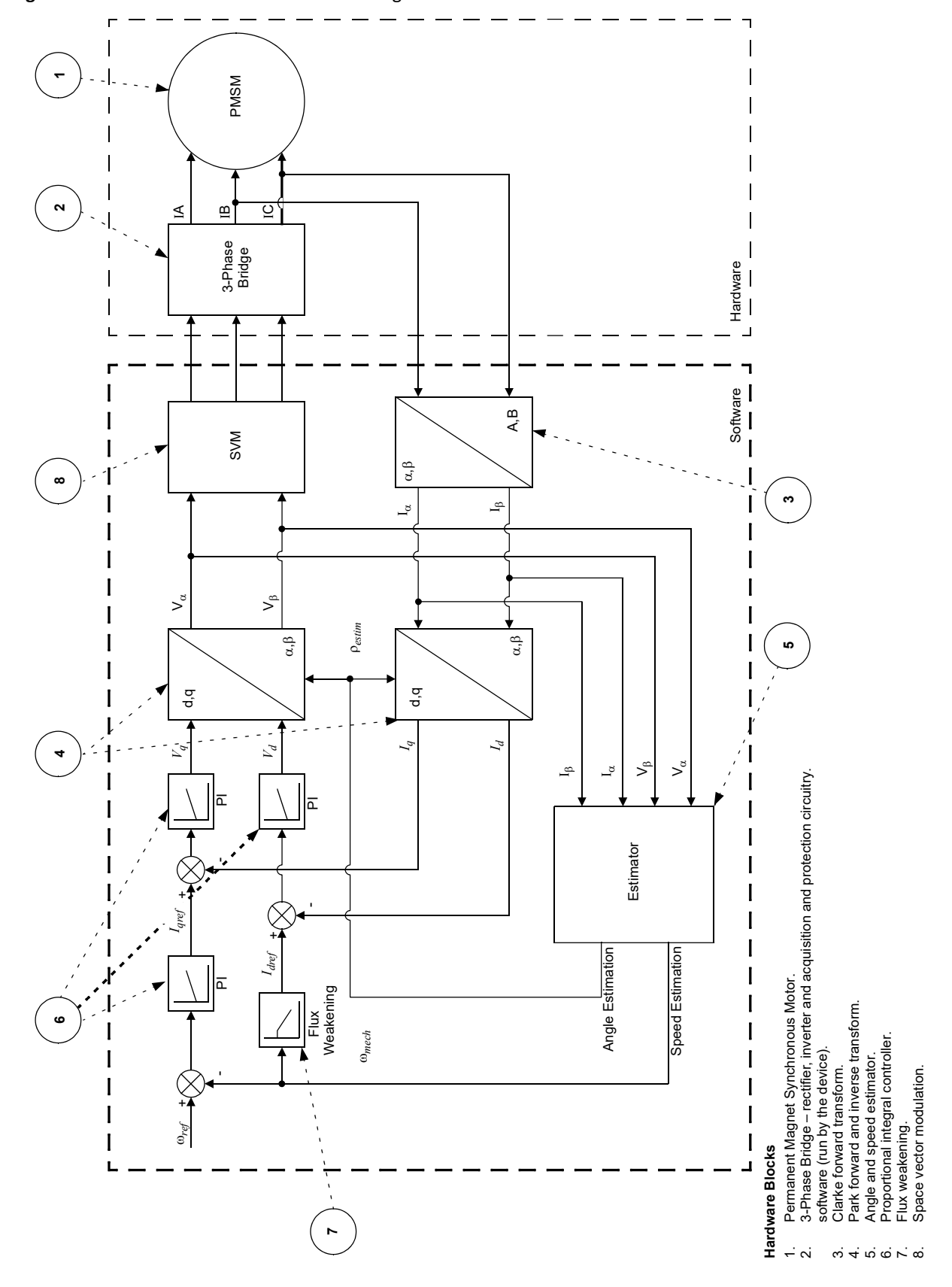
It is beyond the scope of this application note to explain the FOC details; however, the particulars of the new implementation will be covered with respect to the previously indicated application notes.

The control scheme for FOC is illustrated in Figure 1-1. This scheme was implemented and tested using the dsPICDEM™ MCLV-2 Development Board (DM330021-2), which can drive a PMSM motor using different control techniques without requiring any additional hardware.

The control scheme is similar to the one described in application note "AN1292 - Sensorless Field Oriented Control (FOC) for a Permanent Magnet Synchronous Motor (PMSM) Using a PLL Estimator and Field Weakening (FW)" (see References), except for the flux weakening.



Figure 1-1. Sensorless FOC for PMSM Block Diagram





The particularity of the FOC in the PMSM is that the stator's d-axis current reference  $I_{dref}$  (corresponding to the armature reaction flux on d-axis) is set to zero. The rotor's magnets produce the rotor flux linkage,  $\Psi_{PM}$ , unlike ACIM, which needs a constant reference value,  $I_{dref}$ , for the magnetizing current, thereby producing the rotor flux linkage.

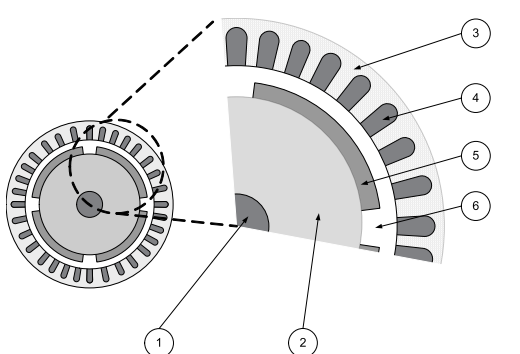
The air gap flux is equal to the sum of the rotor's flux linkage, which is generated by the permanent magnets plus the armature reaction flux linkage generated by the stator current. For the constant torque mode in FOC, the d-axis air gap flux is solely equal to  $\Psi_{PM}$ , and the d-axis armature reaction flux is zero.

On the contrary, in constant power operation, the flux generating component of the stator current,  $I_d$ , is used for air gap flux weakening to achieve higher speed.

In Sensorless control, where no position or speed sensors are needed, the challenge is to implement a robust speed estimator that is able to reject perturbations, such as temperature, electromagnetic noise and so on. Sensorless control is usually required when applications are cost sensitive, where moving parts are not allowed, such as position sensors or when the motor is operated in an electrically hostile environment. However, requests for precision control, especially at low speeds, should not be considered a critical matter for the given application.

The position and speed estimation is based on the mathematical model of the motor. Therefore, the closer the model is to the real hardware, the better the estimator will perform. The PMSM mathematical modeling depends on its topology, differentiating mainly two rotor types: surface-mounted and interior permanent magnet. Each type has its own advantages and disadvantages with respect to the application needs. The proposed control scheme has been developed around a surface-mounted permanent magnet synchronous motor, see Figure 1-2, which has the advantage of low torque ripple and lower price in comparison with other types of PMSMs. The air gap flux for the motor type considered is smooth so that the stator's inductance value,  $L_d = L_q$  (non-salient PMSM), and the Back Electromotive Force (BEMF) is sinusoidal.

Figure 1-2. Surface Mounted PM PMSM Transversal Section



Motor's Transversal Section

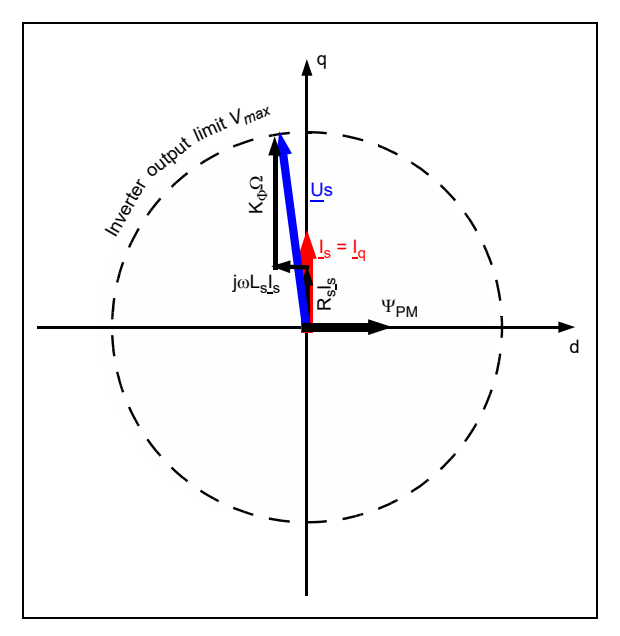
- 1. Rotor shaft.
- 2. Rotor core
- 3. Armature (stator).
- 4. Armature slots with armature windings
- 5. Rotor's permanent magnets.
- 6. Air gap.

The fact that the air gap is large (it includes the surface mounted magnets, being placed between the stator teeth and the rotor core), implies a smaller inductance for this kind of PMSM with respect to the other types of motors with the same dimension and nominal power values. These motor characteristics enable some simplification of the mathematical model used in the speed and position estimator, while at the same time enabling the efficient use of FOC.

When using a surface PMSM, the FOC maximum torque per ampere is obtained by keeping the motor's rotor flux linkage situated at 90 degrees behind the armature generated flux linkage, see Figure 1-3.

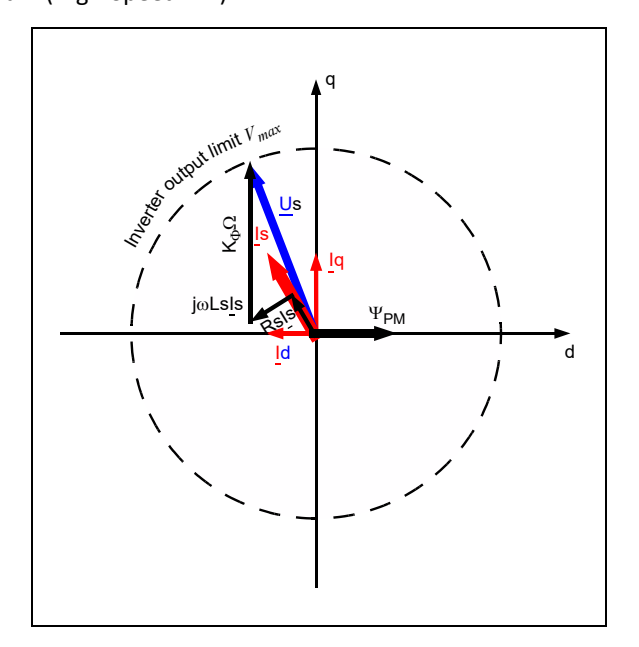


Figure 1-3. FOC Phasor Diagram (Base Speed)



Considering the FOC constant power mode, the flux weakening for the motor considered cannot be done effectively because of the large air gap space, which implies weak armature reaction flux disturbing the rotor's permanent magnets flux linkage. Due to this, the maximum speed achieved should not exceed more than double the base speed for the motor considered for testing. Figure 1-4 illustrates the phasors orientation in constant power, Flux Weakening (FW) mode.

Figure 1-4. FOC Phasor Diagram (High-Speed FW)



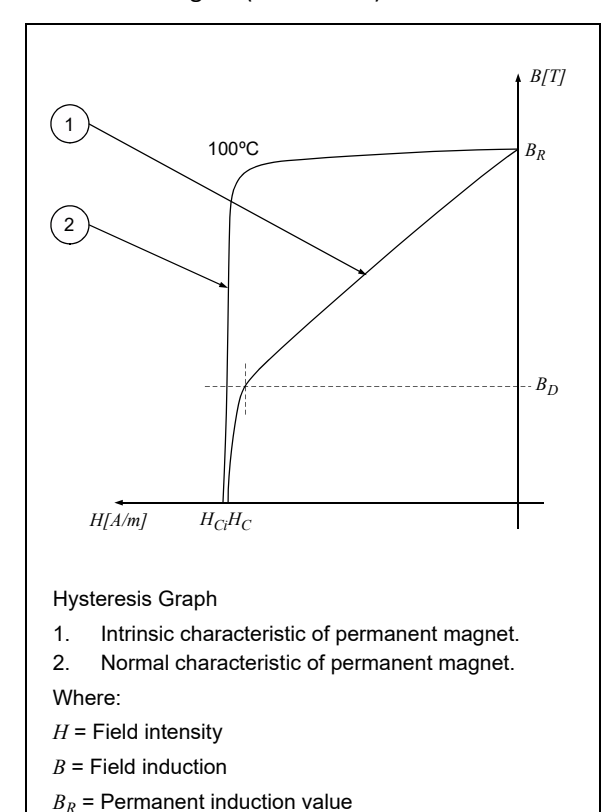




During flux weakening of a Surface Permanent Magnet (SPM) type of PMSM, mechanical damage of the rotor and the demagnetization of the permanent magnets is possible if careful measures are not taken or the motor manufacturer's specifications are not followed. The permanent magnets are usually bonded with an epoxy adhesive or affixed with stainless steel or carbon fiber rings. Beyond the maximum speed indicated by the manufacturer, the magnets could unbind or break, leading to destruction of the rotor along with other mechanical parts attached to the motor's shaft. Demagnetization can be caused by exceeding the knee of flux density, B<sub>D</sub>, for the air gap flux density, as shown in Figure 1-5.

Figure 1-5. Hysteresis Graph of Permanent Magnet (Theoretical)

 $H_C$  = Coercivity  $H_{Ci}$  = Intrinsic coercivity



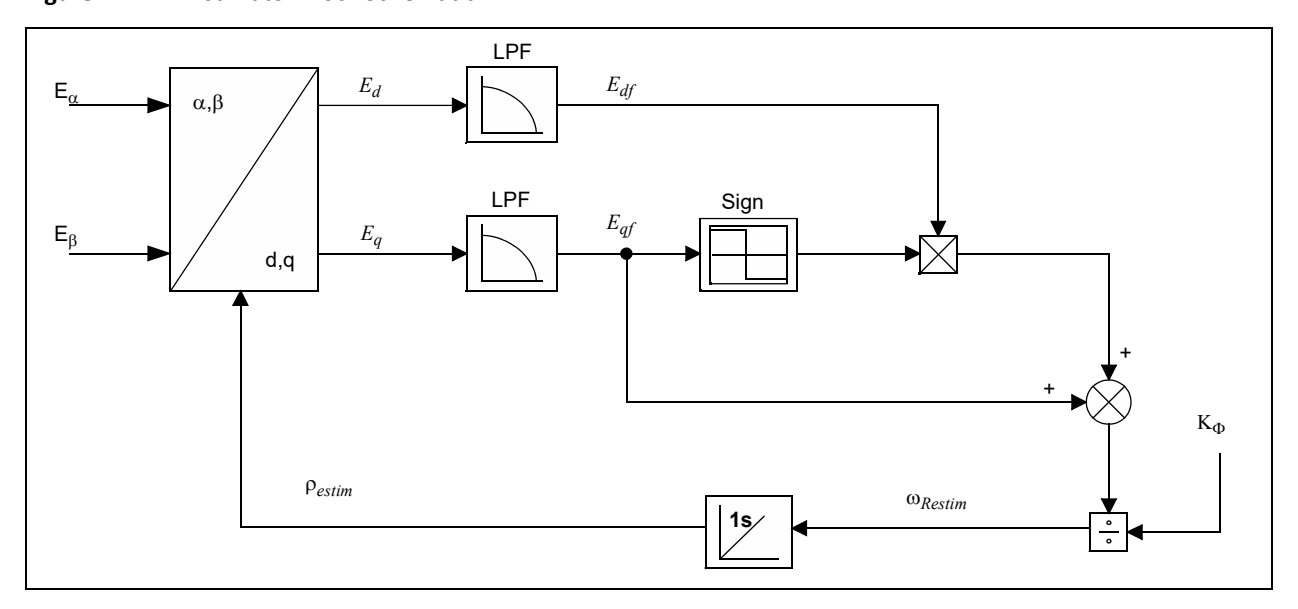


# 2. PLL Type Estimator

The estimator used in this application note is an adaptation of the one presented in "AN1162 - Sensorless Field Oriented Control (FOC) of an AC Induction Motor (ACIM)" (see References), but applied to PMSM motor particularities.

The estimator has PLL structure. Its operating principle is based on the fact that the d-component of the Back Electromotive Force (BEMF) must be equal to zero at a steady state functioning mode. The block diagram of the estimator is shown in Figure 2-1.

Figure 2-1. PLL Estimator Block Schematic



Starting from the closed loop shown in Figure 2-1, the estimated speed ( $\omega_{Restim}$ ) of the rotor is integrated to obtain the estimated angle, as shown in Equation 2-1:

#### Equation 2-1.

$$\rho_{estim} = \int \omega_{Restim} d_t$$

The estimated speed,  $\omega_{Restim}$ , is obtained by dividing the q-component of the BEMF value with the voltage constant,  $K_{\Phi}$ , as shown in Equation 2-2.

#### Equation 2-2.

$$\omega_{Restim} = \frac{1}{K_{\Phi}} \left( E_{qf} - sgn\left(E_{qf}\right) \cdot E_{df} \right)$$

Considering the initial estimation premise (the d-axis value of BEMF is zero at steady state) shown in Equation 2-2, the BEMF q-axis value,  $E_{qf}$ , is corrected using the d-axis BEMF value,  $E_{df}$ , depending on its sign. The BEMF d-q component's values are filtered with a first order filter, after their calculation with the Park transform, as indicated in Equation 2-3.



#### Equation 2-3.

$$E_{d} = E_{\alpha} \cos(\rho_{estim}) + E_{\beta} \sin(\rho_{estim})$$

$$E_{q} = E_{\alpha} \sin(\rho_{estim}) + E_{\beta} \cos(\rho_{estim})$$

With the fixed stator frame, Equation 2-4 represents the stators circuit equations.

#### Equation 2-4.

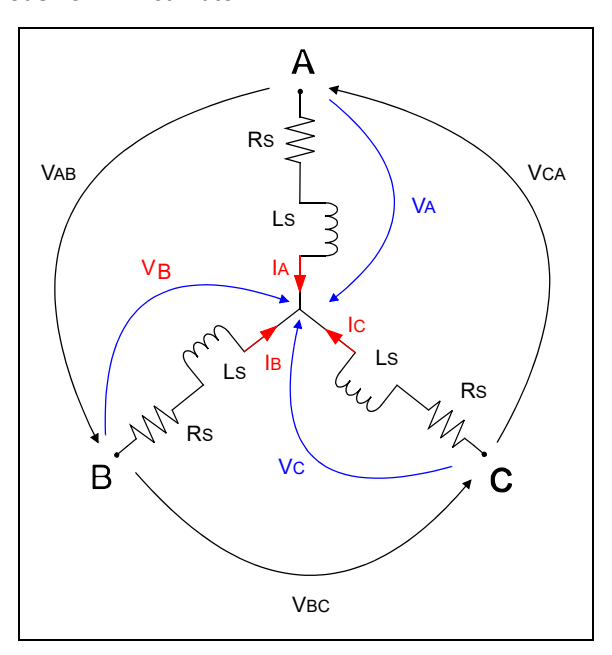
$$E_{\alpha} = V_{\alpha} - R_{S}I_{\alpha} - L_{S}\frac{dI_{\alpha}}{dt}$$

$$E_{\beta} = V_{\beta} - R_{S}I_{\beta} - L_{S}\frac{dI_{\beta}}{dt}$$

In Equation 2-4, the terms containing  $\alpha$  –  $\beta$  were obtained from the three-phase system's corresponding measurements through Clarke transform. L<sub>S</sub> and R<sub>S</sub> represent the per phase stator inductance and resistance, respectively, considering Y (star) connected stator phases. If the motor is  $\Delta$  (delta) connected, the equivalent Y connection phase resistance and inductance should be calculated and used in the equations above.

Figure 2-2 denotes the estimator's reference electrical circuit model. The A, B and C terminals of the motor are connected to the inverter's output terminals. The voltages,  $V_A$ ,  $V_B$  and  $V_C$ , represent the phase voltages applied to the motor's stator windings.  $V_{AB}$ ,  $V_{BC}$  and  $V_{CA}$ , represent the line voltages between the inverter's legs, while the phase currents are  $I_A$ ,  $I_B$  and  $I_C$ .

Figure 2-2. Electrical Circuit Model for PLL Estimator



Taking one step forward concerning the equations implementation in the control system, the voltages  $V_{\alpha}$  and  $V_{\beta}$ , implied in estimator's Equation 2-4 are a previous cycle calculation of the FOC, being fed to the Space Vector Modulation (SVM) block on the previous step of control, but also to the estimator block current step.  $I_{\alpha}$  and  $I_{\beta}$  are Clarke transform results from the phase currents, which are read every estimator cycle.



The resulting  $E_{\alpha}$  and  $E_{\beta}$  values of BEMF are translated to the rotating reference frame of the rotor flux through the Park transform resulting in  $E_d$  and  $E_q$  values, which conform to Equation 2-3. The angle  $\rho_{estim}$ , used in Park transformation is calculated on the previous execution cycle of the estimator. The d-q values of BEMF are then filtered using first order filters, entering the main condition of the estimator, based on  $E_d$  being equal to '0'.

Equation 2-2 reflects the calculation of  $\omega_{Restim}$ , which is the resulting electrical speed. The integrated electrical speed provides the angle ( $\rho_{estim}$ ) between the rotor flux and the  $\alpha$  –  $\beta$  fixed stator frame. In Equation 2-2,  $K_{\Phi}$  denotes the voltage constant as indicated in Table 3-1. The  $K_{\Phi}$  used in the electrical speed computation, is shown in Equation 2-5.

#### Equation 2-5.

MotorEstimParm.qInvKFi represents:

$$\frac{1}{K_{\Phi\_Electrical}} = \sqrt{3} \cdot 2 \cdot \pi \frac{1000}{60 \cdot K_{\Phi}} \cdot P$$

Where:

P = Number of pole pairs and the other inputs indicated previously

The speed feedback is filtered using a first order filter identical with the one used in the BEMF case. The filter's generic form is shown in Equation 2-6:

#### Equation 2-6.

$$y(n) = y(n-1) + K_{filter} \cdot (x(n) - y(n-1))$$

Where:

y(n) = Current cycle filter output

y(n - 1) = Previous cycle filter output

x(n) = Current cycle filter input

K<sub>filter</sub> = Filter constant

The DC type values at the filter's output should be free of noise from the ADC acquisition or high-frequency variations introduced by the software calculations. The filter's tuning depends on how fast the filtered values (BEMF d-q components and electrical speed) can vary, allowing for sufficient bandwidth, which reduces the possibility of useful signal loss. In the case of BEMF dq components, two situations can be identified:

- High speed. In the Flux weakening mode, where their variation is slow due to the lack of sudden torque change or high acceleration ramp.
- Low speed.

The speed variation depends on the mechanical constant of the motor (and the load coupled on the motor's shaft) and the slope of the ramp up or ramp down limits on the speed reference, whichever is faster.



# 3. Tuning and Experimental Results

The algorithm tuning is very straight forward for speeds below the base speed, where the maximum torque mode is applied. Basically, the motor's parameters, measured or indicated by the manufacturer, are added to the configuration file, mc app.h.

The measurement of parameters comprises the rotor's resistance,  $R_S$ , and inductance,  $L_S$ , and the voltage constant,  $K_{\Phi}$ .

The stator resistance and inductance can be measured at the motor's terminals using a precision LCR meter. For Star connected motors, the stator phase resistance ( $R_S$ ) and inductance ( $L_S$ ) values are obtained by dividing the measured resistance and inductance values at the motor terminals by a factor of 2. For Delta connected motors, the stator phase resistance and inductance values are obtained by multiplying the measured resistance and inductance values at the motor terminals by a factor 1.5.

Dividing the stator phase resistance and inductance values of a Delta connected motor by a factor of 3 results in their Star connected motor equivalent phase resistance ( $R_s$ ) and inductance ( $L_s$ ).

This voltage constant,  $K_{\Phi}$ , is indicated by all motor manufacturers; however, it can be measured using a very simple procedure, by rotating the rotor shaft with a constant speed, while measuring the output voltage at the motor's terminals. If the reading is done at 1000 RPM, the alternative voltage measure is a typical RMS value. Multiplying the reading value by the square root of 2 will return the value in  $V_{\text{peak}}/KRPM$ .

For the tested motor parameters, the data provided in Table 3-1 was measured with the procedures described above.

Motor Type	Hurst Motor DMB00224C10002	Units				
Connection type	Υ	_				
L-L Resistance	2.1 · 2	Ohms				
L-L Inductance – 1 kHz	1.92 · 2	mH				
Voltage constant $K_{\Phi}$	7.24	V <sub>peak</sub> /KRPM				
Ambient temperature	22.7	°C				

Table 3-1. Tested Motor Parameters

The two necessary phase currents are read on the two shunts available on the dsPICDEM MCLV-2 Development Board and their values are scaled to the acceptable input range of the ADC module. The overall current scaling factor depends on the gain of the differential Op amp reading the shunt and the maximum value of the current passing through the motor. For example, having a phase current of 4.4A peak and a gain of 75, for a 0.005 Ohms shunt resistor, results in 3.3V present at the ADC input.

With respect to the initial calibration, the startup may be done with load, in which case the open loop ramp parameters need to be tuned.

The open loop tuning parameters include the lock time, the end acceleration speed, and the current reference value. The lock time represents the time necessary for rotor alignment, which depends on the load initial torque and moment of inertia (the larger they are, the larger the lock time value). The end speed of the initial ramp in RPM should be set sufficiently high for the estimator's calculated BEMF to have enough precision, while the time to reach that speed depends on the open loop q-axis current and resistant load attached on the motor's shaft; the larger the load, the longer the time needed for reaching the end reference speed.

The open loop is implemented as a simplification of the closed loop control, where the estimated angle between the rotor flux and the fixed reference frame is replaced by the forced angle used in open loop speedup. The forced angle does not care about the rotor's position, but rather imposing



its position, being calculated as a continuous increment fraction. An additional simplification from the control loop presented in Figure 1-1, is the lack of the speed controller and the current reference for the q-axis being hard-coded.

The q-axis current reference is responsible for the current forced through the motor in the open loop ramp up; the higher the initial load, the higher the current needed, which acts as a torque reference overall.

To keep the algorithm functioning in open loop, thus disabling the closed loop transition for initial tuning purposes, enable the specific code macro definition, as shown in Example 1.

```
Example 1:
#define OPEN_LOOP_FUNCTIONING
```

This is particularly useful for the potential PI controller's recalibration or even some initial transition conditions verifications (such as angle error between the imposed angle and the estimated one, current scaling constant experimental determination), and initial open loop ramp up parameters fine tuning, previous to the closed loop activation.



# 4. Equation-based Flux Weakening

The back-EMF of the motor increases linearly with speed. Therefore, to counter the back-EMF and support the load, the applied voltage increases linearly with speed. The maximum DC bus voltage (V<sub>BUS</sub>) is limited by practical considerations, such as winding insulation, motor safe operating zone. In a SVPWM modulation scheme, the maximum applicable phase voltage is shown in Equation 4-1. For a given PMSM motor and DC bus voltage, the maximum applicable phase voltage is not sufficient to counter the generated back-EMF voltage and support the load beyond the base speed of the motor. To increase the speed of the motor beyond base speed, the generated back-EMF must be reduced, which is achieved by weakening the rotor magnetic flux, and is termed Flux weakening mode.

#### Equation 4-1.

$$V_{PHASE\_MAX_{SVPWM}} = \frac{V_{BUS}}{\sqrt{3}}$$

Equation 4-2 shows the steady state voltage equation of the D-Q axis of the PMSM motor. The q-axis applied voltage,  $V_{qs}$  counteracts the back EMF ( $\omega \cdot \Psi_{PM}$ ) to drive the load at a particular speed.  $V_{qs}$  voltage is limited by maximum DC bus voltage. In order to increase the speed of the motor without increasing the DC bus voltage, the back-EMF must be reduced by lowering the rotor magnet flux linkage,  $\Psi_{PM}$ . However, in a PMSM motor the flux linkage due to the rotor permanent magnets ( $\Psi_{PM}$ ) is constant. Thus, in PMSM motor, flux weakening is achieved by injecting negative current in d-axis (i.e., -i<sub>ds</sub> such that it counteracts the rotor magnet flux linkage,  $\Psi_{PM}$ ).

#### Equation 4-2.

The dynamic d/q-axis voltage equation for the PMSM is:

$$V_d = R_S \cdot i_d - \omega \cdot L_S \cdot i_q + L_S \cdot \frac{di_d}{dt}$$

$$V_q = R_S \cdot i_q + \omega \cdot L_S \cdot i_d + \omega \cdot \Psi_{PM} + L_S \cdot \frac{di_q}{dt}$$

Since  $i_d$  and  $i_q$  are DC values, they become negligible under steady state, and therefore, the voltage equation can be rewritten as:

$$V_{ds} = R_S \cdot i_{ds} - \omega \cdot L_S \cdot i_{qs}$$

$$V_{qs} = R_S \cdot i_{qs} + \omega \cdot L_S \cdot i_{ds} + \omega \cdot \Psi_{PM}$$

Where,

 $V_{ds}$  = steady state d-axis voltage in V

V<sub>qs</sub> = steady state q-axis voltage in V

i<sub>ds</sub> = steady state d-axis current in A

i<sub>qs</sub> = q-axis current in A

 $\omega$  = Target motor electrical speed in rad/sec

L<sub>s</sub> = Motor phase inductance in H

 $R_S$  = Motor phase resistances in  $\Omega$ 



During flux weakening, the negative d-axis current must be injected such that the applied voltage magnitude always lies on the voltage limit circle,  $V_{max}$ , as shown in Figure 1-4. Therefore, the d-axis current,  $i_{ds}$  can be calculated, as shown in Equation 4-3.

#### Equation 4-3.

$$\begin{aligned} V_{qs_{ref}} &= \sqrt{V_{max}^2 - V_{ds}^2} \\ i_{ds_{flux\_weakening}} &= \frac{V_{qs_{ref}} - R_S \cdot i_{qs} - \omega \cdot \Psi_{PM}}{\omega \cdot L_S} \end{aligned}$$

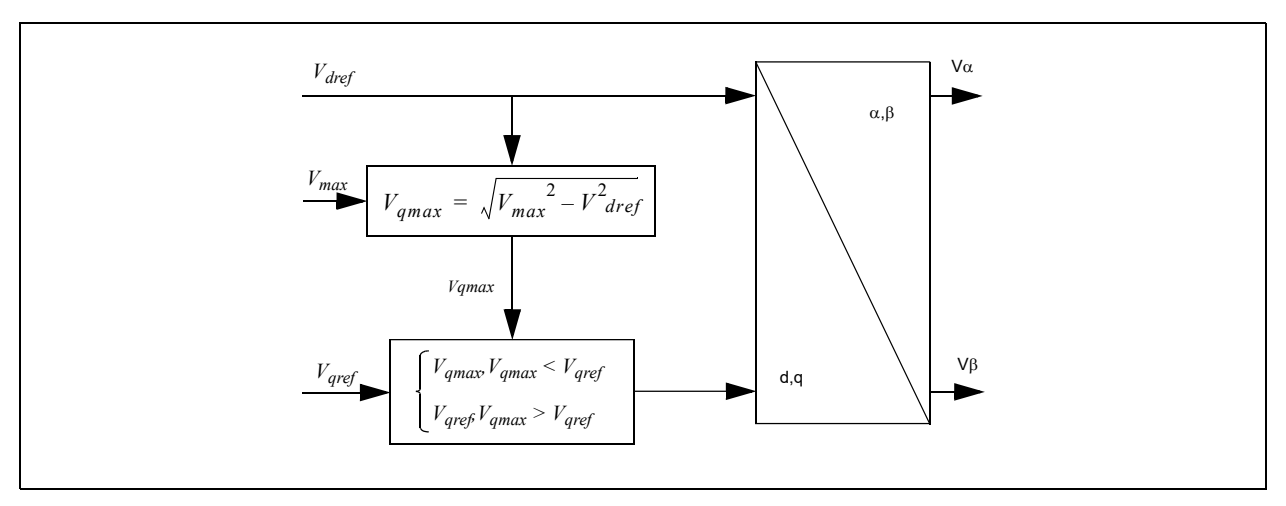
The maximum value of q-axis current is limited during flux weakening in order to ensure that the maximum magnitude of the injected current does not exceed the maximum rated motor current, as shown in Equation 4-4. Therefore, operation in flux weakening causes reduction in torque generating capability.

#### Equation 4-4.

$$lqs\_ref\ max = \sqrt{(I_{motor\_max}^2 - I_{ds_{flux_{weakening}}}^2)}$$

A concern during the Flux Weakening mode is voltage limitation of the inverter. This voltage limitation is translated to the maximum achievable values for d-q current components. If both components would have followed their reference values, their resulting scalar summation value would overlap the maximum value of '1'. Therefore, the maximum current permitted for q-component of the current (the torque component of the current) will result from prioritizing the d-component of the current responsible flux weakening, which is more important due to air gap flux weakening purposes. Figure 4-1 presents this dynamic adjustment translated to the d-q component of the voltages (d-component of voltage prioritizing).

Figure 4-1. Dynamic Voltage Adjustment Block Schematic



Because estimator performance depends drastically on the parameters of the motor, the experimental results keep this premise for the conditions of the measurements. The first dependence of rotor resistance and flux constant of the motor is the temperature. A high torque is obtained using the maximum current input, resulting in high Joule losses, resulting in an increased motor temperature. This has a negative effect on the validity of the estimator's output. The intention



of this application note is not to correct or compensate for the effect of temperature on the estimation. The compensation of parameters with temperature is possible, but it varies considerably from one motor type to another, the working conditions and functional mode. As a consequence, the test results indicated below have a premise that limits the temperature effect on the estimator's output. The time for the achieved torque is limited to one minute of continuous functioning at room temperature, see Table 4-1.

It may be observed that the phase current measured for the last two entries in Table 4-1, corresponding to the flux weakening operation, are higher than the ones immediately preceding them, in normal operation speed.

Table 4-1. Experimental Results Tests with Load

Reference Speed (RPM)	Achieved Speed (RPM)	Load Torque (Nm)	Phase Current (A RMS)
500	500	0.1	1.280
1000	1000	0.09	1.140
1500	1500	0.08	1.035
2000	2001	0.07	0.943
2500	2501	0.04	0.542
3000	3001	0.025	0.56
3500	3504	0.029	1.06
4000	3985	0.03	1.462

**Note:** The experimental test results shown were conducted on the DMB0224C10002 motor.



# 5. Architectural Highlights of 32-bit MCUs for Motor Control Applications

### 5.1 The SAM E70 Family of Devices

#### CPU

- 32-bit Arm® Cortex®-M7 Core 300 MHz (2.14 DMIPS/MHz)
- DSP instruction support (2x DSP performance of Arm Cortex-M4)
- Double-precision Floating Point Unit (FPU) IEEE® 754 Compliant
- Tightly Coupled Memory (TCM) High-speed, Low latency, and deterministic access for timecritical code and data

#### **Analog Features**

- Two dedicated 12-bit ADC modules with dual Sample and Hold (S&H) (i.e., capable of simultaneous sampling of four channels)
- · One on-chip Analog Comparator
- · Two on-chip DAC modules

#### **PWM**

- Up to eight PWM channels capable of generating complimentary PWM with dead-time in edgealigned mode or center-aligned mode
- Two 2-bit gray up/down channels for stepper motor control
- Independent output override for each channel, useful for Trapezoidal control
- Two independent programmable events lines capable of generating precise and synchronized ADC triggers without any software intervention
- Asynchronous Fault inputs allow fast response PWM shutdown under Fault condition without any software intervention
- Spread Spectrum Counter reduces acoustic noise/electromagnetic interference of a PWMdriven motor

#### **Position Sensing**

On-chip Quadrature Decoder (QDEC) – input lines filtering, decoding, timer/counters to read rotor position and speed

# 5.2 The PIC32MK Family of Devices

#### **CPU**

- 32-bit MIPS32® microAptiv™ MCU core, 120 MHz (198 DMIPS)
- DSP-enhanced core
- Double-precision Floating Point Unit (FPU), IEEE 754 Compliant

#### **Analog Features**

- Up to six dedicated 12-bit ADC channels and one shared 12-bit ADC channel
- Up to four on-chip op amp modules
- Up to five on-chip Analog Comparator modules
- Up to three on-chip DAC modules

#### **PWM**

• Up to 12 PWM pairs capable of generating complimentary PWM with dead-time in edge-aligned mode and symmetric/asymmetric center-aligned mode



- PWM channels capable of generating precise and synchronized ADC triggers without any software intervention
- Asynchronous Fault inputs allows fast response PWM shutdown under fault condition without any software intervention

**Position Sensing** 

On-chip QEI interfaces with incremental encoders to obtain rotor mechanical position



# 6. Conclusion

This application note describes a method of flux angle and speed estimation for Permanent Magnet Synchronous Motors. It also describes the equation-based closed loop flux weakening. The main theoretical ideas behind the estimator, equation-based closed loop flux weakening, and the tuning directions are also discussed.

The application described in this document uses support files for the ease of adapting it to other motors. Additionally, using the indicated development hardware platform offered by Microchip for your application can significantly reduce time-to-market.



#### 7. References

- Speed Estimators, Flux Weakening and Efficient Use of SPMSM and IPMSM" Prasad Kulkarni, 20089 MC7, Microchip MASTERs Conference 2016
- The following documents, which are referenced in this document, are available for download from the Microchip web site (www.microchip.com):
  - AN1292 Sensorless Field Oriented Control (FOC) for a Permanent Magnet Synchronous Motor (PMSM) Using a PLL Estimator and Field Weakening (FW) (DSDS01292A): ww1.microchip.com/downloads/en/AppNotes/01292A.pdf
  - AN908 Using the dsPIC30F for Vector Control of an ACIM (DS00908B): ww1.microchip.com/downloads/en/DeviceDoc/00908B.pdf
  - AN1078 Sensorless Field Oriented Control of PMSM Motors (DS01078B): ww1.microchip.com/downloads/aemDocuments/documents/OTH/ApplicationNotes/ ApplicationNotes/01078B.pdf
  - AN1162 Sensorless Field Oriented Control (FOC) of an AC Induction Motor (ACIM) (DS01162A):
    - ww1.microchip.com/downloads/en/Appnotes/01162A.pdf



# 8. Revision History

# 8.1 Revision D (December 2024)

This revision includes the following updates:

• Document migrated to SDL format.

# 8.2 Revision C (August 2018)

This revision includes the following updates:

• Removed Equation 11 and associated text due to test results.

# 8.3 Revision B (September 2017)

This revision includes the following updates:

- The application note reference on the first page was changed to AN1292 "Sensorless Field Oriented Control (FOC) for a Permanent Magnet Synchronous Motor (PMSM) Using a PLL Estimator and Field Weakening (FW)".
- Table 4-1 was updated.
- Minor updates to text were implemented.

# 8.4 Revision A (August 2017)

This is the initial released version of this document.



# **Microchip Information**

#### **Trademarks**

The "Microchip" name and logo, the "M" logo, and other names, logos, and brands are registered and unregistered trademarks of Microchip Technology Incorporated or its affiliates and/or subsidiaries in the United States and/or other countries ("Microchip Trademarks"). Information regarding Microchip Trademarks can be found at https://www.microchip.com/en-us/about/legal-information/microchip-trademarks.

ISBN: 979-8-3371-0355-6

#### **Legal Notice**

This publication and the information herein may be used only with Microchip products, including to design, test, and integrate Microchip products with your application. Use of this information in any other manner violates these terms. Information regarding device applications is provided only for your convenience and may be superseded by updates. It is your responsibility to ensure that your application meets with your specifications. Contact your local Microchip sales office for additional support or, obtain additional support at <a href="https://www.microchip.com/en-us/support/design-help/client-support-services">www.microchip.com/en-us/support/design-help/client-support-services</a>.

THIS INFORMATION IS PROVIDED BY MICROCHIP "AS IS". MICROCHIP MAKES NO REPRESENTATIONS OR WARRANTIES OF ANY KIND WHETHER EXPRESS OR IMPLIED, WRITTEN OR ORAL, STATUTORY OR OTHERWISE, RELATED TO THE INFORMATION INCLUDING BUT NOT LIMITED TO ANY IMPLIED WARRANTIES OF NON-INFRINGEMENT, MERCHANTABILITY, AND FITNESS FOR A PARTICULAR PURPOSE, OR WARRANTIES RELATED TO ITS CONDITION, QUALITY, OR PERFORMANCE.

IN NO EVENT WILL MICROCHIP BE LIABLE FOR ANY INDIRECT, SPECIAL, PUNITIVE, INCIDENTAL, OR CONSEQUENTIAL LOSS, DAMAGE, COST, OR EXPENSE OF ANY KIND WHATSOEVER RELATED TO THE INFORMATION OR ITS USE, HOWEVER CAUSED, EVEN IF MICROCHIP HAS BEEN ADVISED OF THE POSSIBILITY OR THE DAMAGES ARE FORESEEABLE. TO THE FULLEST EXTENT ALLOWED BY LAW, MICROCHIP'S TOTAL LIABILITY ON ALL CLAIMS IN ANY WAY RELATED TO THE INFORMATION OR ITS USE WILL NOT EXCEED THE AMOUNT OF FEES, IF ANY, THAT YOU HAVE PAID DIRECTLY TO MICROCHIP FOR THE INFORMATION.

Use of Microchip devices in life support and/or safety applications is entirely at the buyer's risk, and the buyer agrees to defend, indemnify and hold harmless Microchip from any and all damages, claims, suits, or expenses resulting from such use. No licenses are conveyed, implicitly or otherwise, under any Microchip intellectual property rights unless otherwise stated.

# **Microchip Devices Code Protection Feature**

Note the following details of the code protection feature on Microchip products:

- Microchip products meet the specifications contained in their particular Microchip Data Sheet.
- Microchip believes that its family of products is secure when used in the intended manner, within operating specifications, and under normal conditions.
- Microchip values and aggressively protects its intellectual property rights. Attempts to breach the code protection features of Microchip products are strictly prohibited and may violate the Digital Millennium Copyright Act.
- Neither Microchip nor any other semiconductor manufacturer can guarantee the security of its code. Code protection does not mean that we are guaranteeing the product is "unbreakable".
   Code protection is constantly evolving. Microchip is committed to continuously improving the code protection features of our products.

